Applied and Environmental Microbiology, June 2010, p. 3599–3610 Vol. 76, No. 11
0099-2240/10/$12.00 doi:10.1128/AEM.00058-10

Comparative Transcriptome and Secretome Analysis of Wood Decay Fungi *Postia placenta* and *Phanerochaete chrysosporium*▽†

Amber Vanden Wymelenberg,[1] Jill Gaskell,[2] Michael Mozuch,[2] Grzegorz Sabat,[3] John Ralph,[4] Oleksandr Skyba,[5] Shawn D. Mansfield,[5] Robert A. Blanchette,[6] Diego Martinez,[7] Igor Grigoriev,[8] Philip J. Kersten,[2] and Dan Cullen[2]*

Department of Bacteriology, University of Wisconsin, Madison, Wisconsin 53706[1]; USDA Forest Service, Forest Products Laboratory, Madison, Wisconsin 53726[2]; Genetics and Biotechnology Center, University of Wisconsin, Madison, Wisconsin 53706[3]; Department of Biochemistry and Department of Energy, Great Lakes Bioenergy Research Center, University of Wisconsin, Madison, Wisconsin 53726[4]; Department of Wood Science, University of British Columbia, Vancouver, British Columbia V6T 1Z4, Canada[5]; Department of Plant Pathology, University of Minnesota, St. Paul, Minnesota 55108[6]; Department of Biology, University of New Mexico, Albuquerque, New Mexico 87131[7]; and Department of Energy, Joint Genome Institute, Walnut Creek, California 94598[8]

Received 8 January 2010/Accepted 5 April 2010

Cellulose degradation by brown rot fungi, such as *Postia placenta*, is poorly understood relative to the phylogenetically related white rot basidiomycete, *Phanerochaete chrysosporium*. To elucidate the number, structure, and regulation of genes involved in lignocellulosic cell wall attack, secretome and transcriptome analyses were performed on both wood decay fungi cultured for 5 days in media containing ball-milled aspen or glucose as the sole carbon source. Using liquid chromatography-tandem mass spectrometry (LC-MS/MS), a total of 67 and 79 proteins were identified in the extracellular fluids of *P. placenta* and *P. chrysosporium* cultures, respectively. Viewed together with transcript profiles, *P. chrysosporium* employs an array of extracellular glycosyl hydrolases to simultaneously attack cellulose and hemicelluloses. In contrast, under these same conditions, *P. placenta* secretes an array of hemicellulases but few potential cellulases. The two species display distinct expression patterns for oxidoreductase-encoding genes. In *P. placenta*, these patterns are consistent with an extracellular Fenton system and include the upregulation of genes involved in iron acquisition, in the synthesis of low-molecular-weight quinones, and possibly in redox cycling reactions.

Wood decay basidiomycetes, often categorized as white rot or brown rot fungi, are common inhabitants of forest litter, where they play a key role in carbon cycling (15). White rot fungi degrade all components of plant cell walls, including cellulose, hemicellulose, and lignin. Although unable to grow on lignin alone, these filamentous fungi have the unique ability to degrade a large proportion completely to CO_2 and H_2O. White rot fungi, such as *Phanerochaete chrysosporium*, also employ an array of extracellular hydrolases that attack cellulose and hemicellulose while simultaneously depolymerizing the lignin by oxidative mechanisms (33). Brown rot fungi, exemplified by *Postia placenta*, employ a different approach. Early in the decay process, they rapidly depolymerize cellulose but without concomitant weight loss. As decay progresses, brown rot fungi modify lignin extensively, but the products remain *in situ* as a polymeric residue (40, 59). Brown rot fungi are of considerable economic importance as the principal agents causing the destructive decay of wooden structures.

Although gross patterns of lignocellulose degradation differ substantially, the two decay types probably share at least some mechanisms, because molecular phylogeny, morphology, mating systems, and substrate preferences suggest that brown rot fungi have repeatedly evolved from white rot fungi (21). *P. placenta* and *P. chrysosporium* are members of the Phlebia clade, which lies within the order *Polyporales* (5, 20). Recent comparison of their genomes (36) indicated that the derivation of brown rot fungi is characterized largely by the contraction or loss of multiple gene families that are thought to be important in typical white rot, such as cellulases, lignin peroxidases (LiPs), manganese peroxidases (MnPs), copper radical oxidases (CROs), cellobiose dehydrogenase (CDH), and pyranose-2-oxidase (POX). This general pattern of simplification is consistent with the view that brown rot fungi have acquired novel mechanisms for cellulose depolymerization and lost key components of the white rot lignocellulose-degrading system (57).

Previous microarray studies provided quantitative transcript profiles for *P. chrysosporium* (52) grown in defined medium containing either glucose or microcrystalline cellulose as sole carbon source. The transcriptome of *P. chrysosporium* has also been partially characterized by expressed sequence tag (cDNA) microarrays (28), serial analysis of gene expression (38), and most recently by deep pyrosequencing of cDNAs derived from oak-grown cultures (43). These transcriptome investigations have been complemented by mass spectrometry identification of *P. chrysosporium* proteins in defined (45, 53), semidefined (54), and complex (1, 41, 44) media. Considered together with numerous reports characterizing *P. chrysosporium* glycoside hydrolases (GHs) (reviewed in reference 2), there remains little doubt that hemicellulose and cel-

* Corresponding author. Mailing address: Forest Products Lab, One Gifford Pinchot Drive, Madison, WI 53726. Phone: (608) 231-9468. Fax: (608) 231-9262. E-mail: dcullen@facstaff.wisc.edu.

† Supplemental material for this article may be found at http://aem.asm.org/.

▽ Published ahead of print on 16 April 2010.

lulose degradation involve the concerted action of conventional hydrolytic enzymes.

In contrast, relatively little is known about the mechanism(s) of cellulose degradation by *P. placenta* or by brown rot fungi in general (reviewed in reference 2). Analysis of the *P. placenta* genome revealed a repertoire of genes distinct from those of all known cellulose-degrading microbes (36). The genome completely lacks cellulose-binding domains, and the number of glycosyl hydrolases is relatively low, owing in part to the paucity of cellulases. No exocellobiohydrolases and only two potential β-1,4-endoglucanase genes were identified. One putative endoglucanase (Ppl115648) was shown to be expressed at high levels in medium containing microcrystalline cellulose, relative to levels in glucose-grown mycelia, but it seems unlikely that this endoglucanase alone can account for the efficient cellulose depolymerization by *P. placenta*. Other GHs and/or hypothetical proteins may therefore be necessary for the complete breakdown of cellulose, and a central goal of our investigations was to identify potentially important enzymes by examining transcriptome and secretome patterns in cultures containing ground aspen as the sole carbon source.

Many investigations of the mechanisms employed by white rot and brown rot fungi have suggested the participation of low-molecular-weight oxidants. A hydroxyl radical, generated via the Fenton reaction ($H_2O_2 + Fe^{2+} + H^+ \rightarrow H_2O + Fe^{3+} + OH^{\cdot}$), has been strongly implicated as a diffusible oxidant in brown rot (recent papers on this topic include references 10, 36, and 58) and, to a lesser extent, in white rot (2). To identify specific enzymes and provide insight into mechanisms of lignocellulose degradation, we report here the systematic comparisons of transcriptomes and secretomes of *P. placenta* and *P. chrysosporium* when cultivated on a lignocellulosic substrate.

MATERIALS AND METHODS

Culture conditions and characterization. RNA for microarrays was obtained from *P. chrysosporium* strain RP78 and *P. placenta* strain MAD-698-R (Forest Mycology Center, Forest Products Laboratory, USDA Forest Service) grown in Highley's basal salt medium (23) containing either 0.5% (wt/vol) ball-milled aspen (BMA) or glucose as sole carbon source. Highley's basal medium contains per liter 2 g NH_4NO_3, 2 g KH_2PO_4, 0.5 g $MgSO_4 \cdot 7H_2O$, 0.1 g $CaCl_2 \cdot 2H_2O$, 1 mg thiamine, and 10 ml of a mineral solution [per liter, 1.5 g nitrilotriacetic acid, 3 g $MgSO_4 \cdot 7H_2O$, 0.5 g $MnSO_4 \cdot H_2O$, 1 g NaCl, 0.1 g $FeSO_4 \cdot H_2O$, 0.1 g $CoSO_4$, 0.1 g $CaCl_2$, 0.1 g $ZnSO_4 \cdot 7H_2O$, 0.01 g $CuSO_4$, 0.01 g $AlK(SO_4)_2 \cdot 12H_2O$, 0.01 g H_3BO_3, and 0.01 g $NaMoO_4 \cdot 2H_2O$]. Aliquots of 250 ml of medium in 2-liter Erlenmeyer flasks were inoculated with approximately 10^7 *P. chrysosporium* spores or with *P. placenta* mycelia scraped from the surface of potato dextrose agar. Unless otherwise specified, cultures of *P. chrysosporium* and *P. placenta* were harvested after 5 days on a rotary shaker (150 rpm) at 37°C or room temperature, respectively.

Culture supernatants from all media were tested for lignin peroxidase (50), manganese peroxidase (56), glyoxal oxidase (31, 32), and cellobiose dehydrogenase (3) enzyme activities. *P. placenta* has none of the corresponding genes and, as expected, no activities were detected. In the case of *P. chrysosporium*, these 5-day cultures are too early for significant lignin degradation, and no peroxidase or glyoxal oxidase activity was observed. The BMA-grown *P. chrysosporium* cultures also had no detectable cellobiose dehydrogenase activity. Oxalate concentrations (25) were low (<50 μM) in BMA culture filtrates of both species.

Expression microarrays. From a data set of 10,004 unique *P. chrysosporium* gene predictions, each Roche NimbleGen array (Madison, WI) featured 12 unique 60-mer probes per gene, all in triplicate. (Seven gene models composed mostly of repetitive DNA were represented by only 2 to 11 60-mers.) The *P. placenta* arrays were based on 12,438 gene models, with 10 unique 60-mers per allele, again all in triplicate. Complete design details for *P. chrysosporium* and *P. placenta* Roche NimbleGen arrays are available under platforms GPL8022 and GPL7187, respectively, within the Gene Expression Omnibus (GEO; http://www.ncbi.nlm.nih.gov/geo/index.cgi).

For each of the four combinations of species and medium (BMA-*P. placenta*, BMA-*P. chrysosporium*, glucose-*P. placenta*, and glucose-*P. chrysosporium*), total RNA was purified from triplicate cultures. In short, cultures were harvested by filtering through Miracloth (Calbiochem, EMD Biosciences, Gibbstown, NJ), squeeze dried, and snap-frozen in liquid nitrogen. Pellets were stored at −80°C until use. Extraction buffer was prepared by combining 10 ml of 690 mM sodium *para*-aminosalicylate (Sigma-Aldrich, St. Louis, MO) with 10 ml of 56 mM sodium tri-isopropyl naphthalene sulfonate (Sigma-Aldrich) and placed on ice. To this was added 5 ml of 5× RNB (1.0 M Tris, 1.25 M NaCl, 0.25 M EGTA). The pH of the 5× RNB was adjusted to 8.5 with NaOH. The mixture was kept on ice and shaken just before use.

Frozen fungal pellets were ground to a fine powder with liquid nitrogen in an acid-washed, prechilled mortar and pestle. The ground mycelia were transferred to Falcon 2059 tubes (VWR International, West Chester, PA), and extraction buffer was added to make a thick slurry. The samples were vortexed vigorously and placed on ice until all samples were processed. A one-half volume of Tris-EDTA (TE)-saturated phenol (Sigma-Aldrich) and a ¼ volume of chloroform (Sigma-Aldrich) were added to each sample and samples were again vortexed vigorously. Samples were spun at 2,940 × *g* in a fixed-angle rotor for 5 min. The aqueous layer was removed to a new tube, and phenol-chloroform extractions were repeated until the interface between the aqueous and organic layers was clear. The final aqueous extractions were placed in clean 2059 tubes, to which was added a 0.1 volume of 3 M sodium acetate, pH 5.2 (diethyl pyrocarbonate treated), and 2 volumes of absolute ethanol. The tubes were shaken vigorously and stored overnight at −20°C.

The tubes were spun for 1 h at 2,940 × *g*, the supernatants were decanted, and the pellets were resuspended in 4 ml of RNase-free H_2O. Total RNA was purified using the RNeasy Maxi kit (Qiagen, Valencia, CA) according to the manufacturer's protocol. RNAs were eluted from the RNeasy spin columns using two spins, for a final volume of 2 ml. The eluted RNAs were ethanol precipitated and stored overnight at −20°C. The RNAs were spun for 1 h at 2,940 × *g*, washed once with 70% ethanol, and resuspended in 50 to 100 μl of RNase-free H_2O. Three biological replicates per medium were used (12 separate arrays).

RNA was converted to double-stranded cDNA and labeled with the Cy3 fluorophore. In brief, 10 μg of total RNA was incubated with 1× first-strand buffer, 10 mM dithiothreitol (DTT), 0.5 mM deoxynucleoside triphosphates (dNTPs), 100 pM oligo T7 $d(T)_{24}$ primer, and 400 U of SuperScript II (Invitrogen) for 60 min at 42°C. Second-strand cDNA was synthesized by incubation with 1× second-strand buffer, 0.2 mM dNTPs, 0.07 U/μl DNA ligase (Invitrogen), 0.27 U/μl DNA polymerase I (Invitrogen), 0.013 U/μl RNase H (Invitrogen), at 16°C for 2 h. Immediately following this incubation, 10 U of T4 DNA polymerase (Invitrogen) was added for an additional 5-min incubation at 16°C. Double-stranded cDNA was treated with 27 ng/μl of RNase A (EpiCenter Technologies) for 10 min at 37°C. Treated cDNA was purified using an equal volume of phenol-chloroform-isoamyl alcohol (Ambion), ethanol precipitated, washed with 80% ethanol, and resuspended in 20 μl of water. One microgram of each cDNA sample was amplified and labeled with 1 unit per μl of Klenow fragment (New England BioLabs) and 1 optical density unit of Cy3 fluorophore (TriLink Biotechnologies, Inc.) for 2 h at 37°C. Array hybridization was carried out by Roche NimbleGen (Iceland) using 6 μg of labeled cDNA suspended in NimbleGen hybridization solution for 17 h at 42°C. Arrays were scanned on the Axon 4000B scanner (Molecular Dynamics), and data were extracted from the scanned image using NimbleScan v2.4. The DNASTAR ArrayStar v2.1 software (Madison,WI) was used to quantify and visualize data. Analyses were based on three biological replicates per culture medium. Quantile normalization and robust multiarray averaging (RMA) (26) were applied to the entire data set. Scatter plots of results are shown in Fig. S1 in the supplemental material. Unless otherwise specified, expression levels are based on $\log_2$ values, and significant differences in expression were determined using the moderated *t* test (48) with the false discovery rate (4) threshold set at $P < 0.001$. Newly acquired data can be viewed/downloaded together with previously described microarray results (36, 52) under NCBI GEO design platforms GPL8022 and GPL7187 for *P. chrysosporium* and *P. placenta*, respectively.

Competitive reverse transcription-PCR (RT-PCR) was used to quantify transcripts of *P. placenta* genes encoding three copper radical oxidases, two laccases, two glucose oxidases, and a secreted FAD-containing oxidoreductase. Gene-specific primers and amplicon information are listed in Table S3 of the supplemental material. Quantitative RT-PCR confirmation of *P. chrysosporium* microarrays was previously reported (52).

Mass spectrometry. Soluble extracellular protein was concentrated from culture filtrates as previously reported (53, 54). Following SDS-PAGE fractionation,

in-gel digestion and mass spectrometric analysis were performed on an LC/MSD Trap SL spectrometer (Agilent, Palo Alto, CA) as described elsewhere (www.biotech.wisc.edu/ServicesResearch/MassSpec/ingel.htm). An in-house licensed Mascot search engine (Matrix Science, London, United Kingdom) identified peptides using the 10,048 and 17,173 gene models in the v2.1 *P. chrysosporium* (53) and in the *P. placenta* (36) data sets, respectively. Mascot scores of ≥40 were considered highly significant.

A second approach eliminated SDS-PAGE fractionation and instead precipitated total protein from 200-ml culture filtrates by direct addition of solid trichloroacetic acid (TCA) to 10% (wt/vol). Following overnight storage at −20°C, the precipitate was centrifuged and the pellet washed several times with cold acetone. Pelleted proteins were resolubilized and denatured in 50 μl of 8 M urea–50 mM NH_4HCO_3 for 10 min and then diluted to 250 μl for tryptic digestion with 12.5 μl of 25 mM DTT, 12.5 μl acetonitrile (ACN), 155 μl Milli-Q water, and 20 μl trypsin solution (100 ng/μl Trypsin Gold [Promega Corp.] in 25 mM NH_4HCO_3). Digestion was conducted in two stages, first for 2 h at 42°C and then an additional 20 μl of trypsin solution was added and incubated overnight at 35°C. Reactions were terminated by acidification with 2.5% trifluoroacetic acid (TFA) to a 0.4% final concentration. Peptides generated from digestion were analyzed by nano-LC-MS/MS using the Agilent (Palo Alto, CA) 1100 nanoflow system connected to a hybrid linear ion trap-orbitrap mass spectrometer (LTQ-Orbitrap; Thermo Fisher Scientific, San Jose, CA) equipped with a nanoelectrospray ion source. Capillary high-performance liquid chromatography (HPLC) was performed using an in-house-fabricated column with an integrated electrospray emitter essentially as previously described (35) but using 360-μm by 75-μm fused silica tubing. The column was packed with 5 μm of C_{18} particles (Column Engineering, Ontario, CA) to approximately 12 cm. Sample loading (8 μl) and desalting were achieved using a trapping column in line with the autosampler (Zorbax 300SB-C_{18}; 5 μM; 5 by 0.3 mm; Agilent). HPLC solvents were as follows: loading solvent, 1% (vol/vol) ACN, 0.1 M acetic acid; solvent A, 0.1 M acetic acid in water; solvent B, 95% (vol/vol) acetonitrile, 0.1 M acetic acid in water. Sample loading and desalting were performed at 10 μl/min with the loading solvent delivered from an isocratic pump. Gradient elution was performed at 200 nL/min and by increasing the percentage of solvent B in solvent A from 0 to 40 in 200 min, 40 to 60 in 20 min, and 60 to 100 in 5 min. The LTQ-Orbitrap was set to acquire MS/MS spectra in data-dependent mode as follows: MS survey scans from *m*/*z* 300 to 2,000 were collected in profile mode at a resolving power of 100,000. MS/MS spectra were collected on the five most abundant signals in each survey scan. Dynamic exclusion was employed to increase dynamic range and maximize peptide identifications. This feature excluded precursors up to *m*/*z* 0.55 below and *m*/*z* 1.05 above previously selected precursors. Precursors remained on the exclusion list for 15 s. Single charged ions and ions for which the charge state could not be assigned were rejected from consideration for MS/MS. Using the above-mentioned protein databases, the MS/MS spectra were analyzed using the in-house Sequest search engine (version 27, revision 13; ThermoFinnigan, San Jose, CA). Sequest searches were done with a fragment ion mass tolerance of 0.50 Da, parent ion tolerance of 2.5 Da, and methionine oxidation as variable modification. Scaffold (version 2_05_02; Proteome Software Inc., Portland, OR) was used to validate MS/MS-based peptide and protein identifications. Unless otherwise specified, protein identifications were accepted if they contained at least two identified peptides and if protein probabilities exceeded 95.0% as determined by the Protein Prophet algorithm (39).

Throughout this report, protein similarity scores are based on the Smith-Waterman algorithm (47) using the BLOSUM62 matrix. *P. chrysosporium* and *P. placenta* protein model identification numbers are preceded by Pchr and Ppl, respectively. Detailed information for each protein can be directly accessed by appending the model number to the following strings: http://genome.jgi-psf.org/cgi-bin/dispGeneModel?db=Phchr1&id=X or http://genome.jgi-psf.org/cgi-bin/dispGeneModel?db=Pospl1&id=X, where X is the one- to five-digit model number for *P. chrysosporium* or *P. placenta*, respectively. (Alternatively, access can be obtained via search pages of the genome portals by entering protein ID numbers under Gene Models.) We assigned a function or a "putative" function only when supported by direct experimental evidence or when comparisons to known proteins revealed conserved catalytic features and/or significant alignment scores (bit scores of >150) to known proteins within the Swiss-Prot database. All other proteins were designated hypothetical, and those with significant amino acid similarity (bit scores of >150) to other conceptual translations within GenBank were considered conserved hypothetical proteins.

Microarray data accession numbers. All MIAME-compliant (7) microarray expression data have been deposited in NCBI's Gene Expression Omnibus and are accessible through GEO series accession numbers GSE14736 and GSE12540 for *P. chrysosporium* and *P. placenta*, respectively.

TABLE 1. Gene expression summary for *P. chrysosporium* and *P. placenta* after 5 days of growth in medium containing ball-milled aspen as sole carbon source

Feature	No. of genes identified	
	P. chrysosporium	*P. placenta*
Gene models[a]	10,048	17,173 (12,227)
Microarray target genes	10,004	12,438
Proteins by LC-MS/MS	73	67
Transcript and/or extracellular proteins accumulating in aspen cultures[b]		
Total	77	160
Glycoside hydrolases	33	33
Hypotheticals	15	49
Oxidoreductases	4	21

[a] Based on gene predictions previously described (36, 37, 53). The parenthetical number refers to the predicted number of unique alleles within the parental dikaryon strain of *P. placenta*.

[b] Number of genes whose transcripts accumulated >2-fold ($P < .001$) and/or whose predicted peptides were identified with Mascot scores of >40.

RESULTS

Of the 12,438 *P. placenta* models represented on our microarrays (Table 1), 8,871 were BlastP matched to *P. chrysosporium* proteins with pairwise identities ranging from 28% to 100% (e-values of $<10^{-5}$; scores of >79) (see Table S1 in the supplemental material for a complete listing of Smith-Waterman scores, e-values, and alignment parameters). Due to gene multiplicity and/or allelism within the *P. placenta* protein set, a single *P. chrysosporium* model was often the best "hit" for multiple *P. placenta* protein models. The total number of unique *P. chrysosporium* models matching the *P. placenta* data set was 5,538, approximately 55% of the total *P. chrysosporium* models.

The *P. placenta* expression microarrays identified numerous genes whose transcripts levels differed substantially between glucose- and BMA-containing media. Transcripts corresponding to 253 *P. placenta* gene models accumulated >2-fold in either BMA or glucose medium. Of these, 173 accumulated >2-fold in BMA relative to glucose and, in 145 cases, this upregulation in BMA was highly significant ($P < 0.001$). Transcripts of 80 *P. placenta* genes accumulated >2-fold in glucose medium, and 48 of these showed highly significant increases relative to BMA. The *P. placenta* microarrays include 12,438 targets (Table 1), a design based largely on an imperfect computational deletion of allelic variants (36). Careful manual inspection of the 253 regulated "genes" revealed the presence of both alleles for three of these genes. Taking these adjustments into account, 250 *P. placenta* genes were regulated >2-fold. Of the 250 genes, 190 were significantly regulated ($P < 0.001$), with 142 upregulated in BMA and 48 upregulated in glucose medium.

The overall number of regulated *P. chrysosporium* genes, 296, was not dramatically different from the *P. placenta* microarray results. However, variance between the replicated *P. chrysosporium* cultures was slightly higher than *P. placenta* cultures, and consequently only 65 genes showed significance at our stringent threshold of $P < 0.001$. Of these, transcripts of 57 genes accumulated in BMA, while only 8 genes increased in

the glucose medium. The *P. chrysosporium* v2 gene models are not complicated by allelism, although we could not distinguish between duplications or possible assembly errors for two of the BMA-upregulated genes (*gly74b* models Pchr134556 and Pchr28013 and *cel7F*/*G* models Pchr9702 and Pchr129072). Scatter plots graphically illustrate transcript levels of all genes (see Fig. S1 in the supplemental material), and complete microarray data are available under GEO accession numbers GSE14736 (*P. chrysosporium*) and GSE12540 (*P. placenta*).

Transcript levels in BMA medium were roughly correlated among putative orthologs in the two species (correlation coefficient, 0.223; $n = 8{,}799$ matched pairs) but substantial variation in gene content, gene regulation, and gene expression levels were apparent. For example, of the above-mentioned 190 *P. placenta* genes regulated >2-fold ($P < 0.001$) in BMA, 19 had no apparent homologs in *P. chrysosporium*. Fourteen of these *P. placenta*-specific genes were upregulated in BMA medium, while transcripts of five accumulated in glucose medium. Focusing on the remaining 171 (190 minus 19) regulated *P. placenta* genes with orthologs in *P. chrysosporium*, only 30 (~18%) showed a similar pattern of regulation in the two species, and 8 showed the opposite pattern. Among the latter were genes potentially involved in aromatic compound metabolism (phenylalanine ammonia lyase and aldehyde dehydrogenase) and in iron homeostasis (ferroxidase and iron permease). In *P. placenta*, these genes were upregulated in BMA medium, whereas the *P. chrysosporium* homologs were more highly expressed in glucose medium.

High-scoring peptides corresponding to 67 *P. placenta* protein models and 79 *P. chrysosporium* models were detected by MS/MS analysis of extracellular filtrates from BMA cultures. The LTQ Orbitrap analysis of TCA-precipitated samples identified considerably more proteins relative to SDS-PAGE fractionation and analysis on the Agilent LC/MSD Trap SL spectrometer. Seventy-three *P. chrysosporium* proteins were identified by the former, while only 30 proteins were identified by the latter method. The results were even more pronounced for *P. placenta*, where the number of proteins increased from 19 to 63 using TCA precipitation and the Orbitrap instrument. It is likely that the increased number of identified proteins was due to instrument sensitivity, but sample preparation also may have played some role. The identity and complete data for all 146 proteins are presented in Tables S1 and S2 in the supplemental material.

Regulated and highly expressed *P. chrysosporium* genes. *P. chrysosporium* and *P. placenta* exhibited distinct patterns of glycoside hydrolase expression. Among the 35 *P. chrysosporium* genes whose transcripts accumulated >4-fold ($P < 0.001$) in BMA, 22 could be assigned to a glycosyl hydrolase family (Fig. 1) (9; http://www.cazy.org/). Peptides corresponding to 12 of these were identified in culture filtrates. Exocellobiohydrolase CBHI (GH7 models Pchr137372 and Pchr137216) and exocellobiohydrolase CBHII (GH6 model 133052) were expressed at relatively high levels and substantially upregulated in BMA relative to glucose (Fig. 1). The absence of CBH genes in *P. placenta* was previously noted (36). Similarly, *P. placenta* lacks homologs of significantly upregulated genes within the GH74 (Pchr134556, Pchr138266, and Pchr28013) and GH11 (Pchr133788) families. The latter gene likely encodes an endoxylanase, while the GH74 family is too functionally diverse to assign function.

The *P. chrysosporium* genes corresponding to functionally characterized endoglucanases EG28 (Pchr8466; *cel12A*), EG44 (Pchr4361; *cel5B*), and EG38/36 (Pchr6458; *cel5A*) (19, 51) were also highly expressed and upregulated. High transcript levels and significant peptide scores were also observed for Pchr7048 (*cel12B*), a likely GH12 endoglucanase based on its similarity to *cel12A*. The putative *P. placenta* homologs to *cel12A*/*B* and *cel5A*, Ppl121191 and Ppl117690, respectively, were also highly expressed in BMA but did not exhibit significant transcript accumulation relative to glucose medium. As commonly observed for endoglucanases, Pchr4361 (*cel5B*) and Pchr6458 (*cel5A*) each contain a cellulose binding domain (carbohydrate binding module family 1 [CBM1]) and, as previously noted (36), such substrate binding modules are absent from the *P. placenta* genome.

Transcripts of three putative *P. chrysosporium* GH61-encoding genes accumulated >4-fold in BMA, and corresponding peptides were identified for the dramatically upregulated *cel61B* gene (Pchr121193) (Fig. 1). The *P. chrysosporium* genome contains at least 13 GH61 genes, whereas *P. placenta* has only 2 clear representatives of this family, Ppl135008 and Ppl126811 (36). The *P. placenta* genes are expressed at relatively low levels in BMA. Although often referred to as cellulases or even endoglucanases, the precise function(s) of GH61s is unclear (30).

Excluding the GH11s, a xylanase family absent from the *P. placenta* genome, several genes broadly defined as hemicellulases or pectinases are similarly regulated in the two fungi. Thus, upregulated *P. chrysosporium* genes encoding putative α-galactosidase, polygalacturonase, rhamnogalactosidase, mannosidase, xylanase, and β-D-xylosidase are also recognizable in the *P. placenta* data set, and their transcripts accumulate to some extent in BMA medium (Fig. 1). In contrast, the *P. chrysosporium* gene encoding a putative carbohydrate active esterase (CE1), Pchr126075, is likely involved in hemicellulose degradation, but no similar sequences were detected within the *P. placenta* genome. The putative *P. chrysosporium* glucuronyl esterase, Pchr6482, is highly conserved among various cellulolytic microbes (14). Members of a new family of esterases (CE15s), Pchr6482 and Pchr130517, may hydrolyze ester linkages between glucuronoxylans and lignin (13, 14). The corresponding *P. placenta* gene, Ppl95582, is expressed at relatively low levels and shows only a modest increase in transcript accumulation in BMA medium.

The roles of several highly regulated *P. chrysosporium* genes are unknown, particularly those encoding hypothetical proteins. Of the hypothetical proteins listed in Fig. 1, transcripts of three accumulated in glucose medium and another three accumulated in BMA medium. Of the latter, Pchr131440 features a 5′ CBM1 domain, suggesting a direct interaction with cellulose or hemicelluloses. Beyond these hypothetical proteins, we observed increased transcripts of genes encoding cellobiose dehydrogenase (CDH; Pchr11098) and aldose-1-epimerase (Pchr138479) in BMA medium. As noted previously (54), the precise function of these enzymes is uncertain, but they may be physiologically connected through the generation of the β-anomer of cellobiose, the preferred substrate of CDH (22). Irrespective of the impressive transcript levels, neither

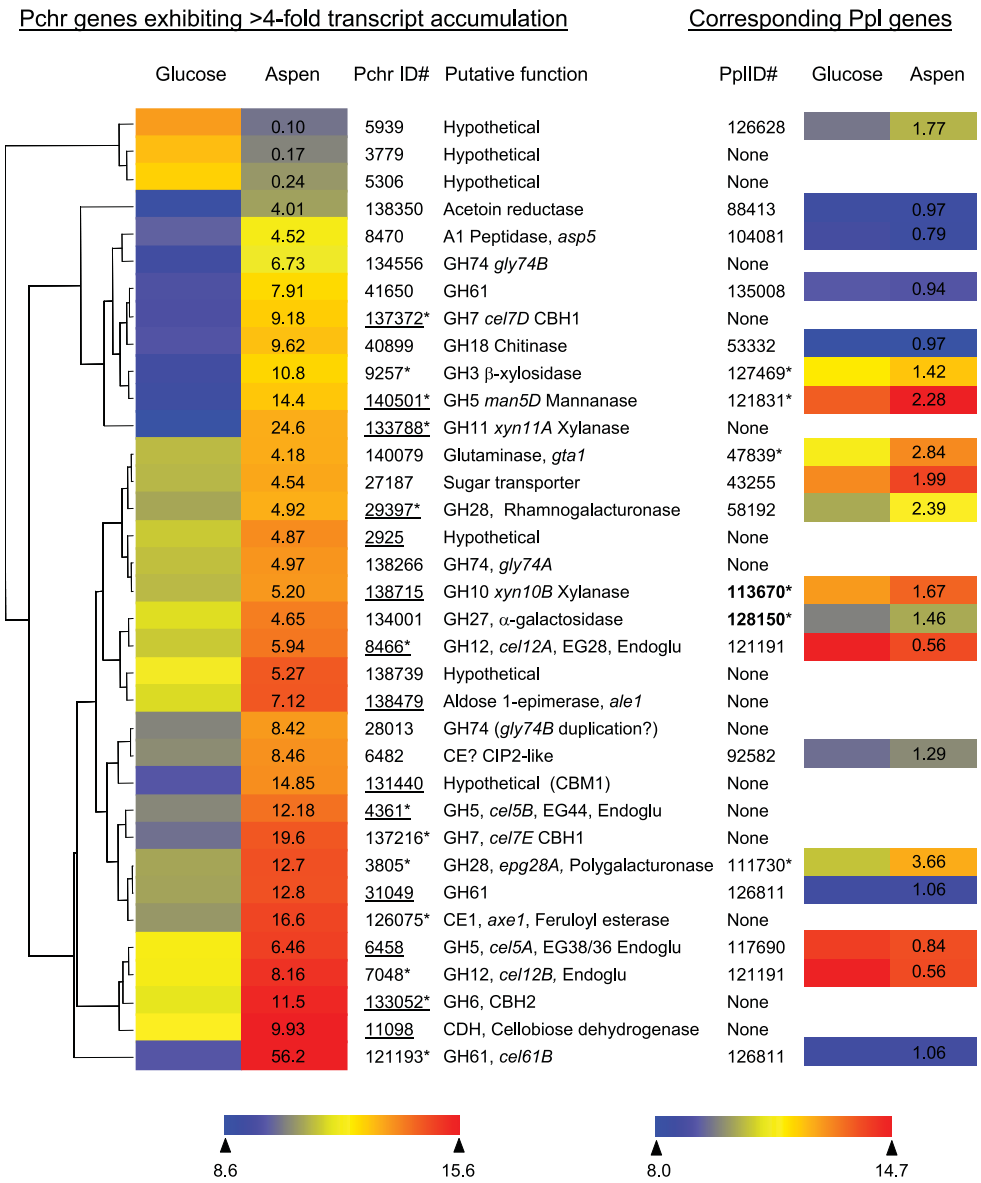

FIG. 1. Heat map showing hierarchical clustering of *Phanerochaete chrysosporium* genes exhibiting highly significant ($P < 0.001$) accumulation of transcripts in aspen-grown versus glucose-grown cultures. Numbers within boxes indicate the fold difference in transcripts for aspen versus glucose cultures. Only those *P. chrysosporium* genes exceeding a 4-fold difference are shown. Underlined *P. chrysosporium* models correspond to genes with >50 cDNA tags in medium containing powdered oak (43). On the right, a heat map shows transcript levels of the most closely related *P. placenta* sequences or, in the absence of a clear homolog, labeled as "None." Protein IDs followed by asterisks correspond to peptides unambiguously identified by LC-MS/MS in filtrates from aspen-grown cultures. The $\log_2$-based scales below maps are calibrated to the data shown above. Boldface denotes models in need of editing: GH10 xylanase model Ppl113670 has been superceded by an annotated preferred version, Ppl134783, which shows less pronounced upregulation (1.10) with a $\log_2$ signal of 11.3. GH27 α-galactosidase model Ppl128150 has been superceded by annotated preferred version Ppl13470, which shows more pronounced upregulation (3.08) with a $\log_2$ signal of 14.4 (Table 3; see also Table S1 in the supplemental material for detailed data).

CDH nor aldose epimerase was detected by mass spectrometry, and no CDH activity was measured in culture filtrates.

With the exception of CDH and a putative acetoin dehydrogenase (Pchr138350), relatively few *P. chrysosporium* oxidoreductase genes were highly regulated under the conditions employed (Fig. 1). Relaxing thresholds for transcript regulation (from 4- to 2-fold) and for the false detection rate (from $P < 0.001$ to $P < 0.01$) still only revealed 10 oxidoreductase genes upregulated in BMA medium (Table 2). Another four putative oxidoreductases were matched to MS/MS-derived peptide sequences (Table 2). Based on structure and well-established biochemistry (60), the FRE-like iron reductase (Pchr1139) and the cellulose binding cytochrome b_{562} (Pchr147) are likely involved in iron reduction. The latter gene has no homolog within *P. placenta*, and the former corresponds to a *P. placenta* gene with relatively low transcript levels in BMA medium ($\log_2$ signal of 10.2). Alcohol oxidase protein models Pchr126879 and Ppl118723 are highly conserved in *P.*

TABLE 2. *P. chrysosporium* genes encoding putative oxidoreductases upregulated >2-fold in BMA medium relative to glucose medium or matched to MS/MS-derived peptide sequences[a]

Phanerochaete chrysosporium						*Postia placenta*							
Model	Putative function	Signal (log_2) in:		Ratio	*P* value	Model	Allele	Pairwise alignment		Signal (log_2) in:		Ratio	*P* value
		Glu	BMA					% ID	Score	Glu	BMA		
11098	Cellobiose dehydrogenase	12.30	15.61	9.93	<0.001	None							
138350	Acetoin dehydrogenase	8.82	10.83	4.01	<0.001	88413	110831	75	1,035	8.37	8.33	0.97	0.521
6771	Oxidoreductase	10.09	11.71	3.09	0.00160	49605	61601	76	1,544	10.07	11.41	2.53	<0.001
41616	Aldo/keto reductase	10.37	11.93	2.96	0.00406	None							
147	Cytochrome b_{562} + CBM1	12.22	13.62	2.64	<0.001	None							
10221	Alcohol dehydrogenase	10.73	12.11	2.60	0.01050	None							
10957	Peroxidase LiPA	9.58	10.92	2.54	0.02240	None							
121806	Peroxidase LiPH	10.95	12.20	2.38	0.00352	None							
1139	FRE-like iron reductase	12.65	13.88	2.35	0.00331	130043	130030	36	635	9.90	10.17	1.20	0.0349
38849	P450	11.72	12.88	2.24	<0.001	None							
126879	Alcohol oxidase*	13.77	14.74	1.97	0.020	118723	129841	88	3090	11.76	14.44	6.43	<0.001
124398	Catalase*	14.24	14.90	1.59	0.004	114720	123169	73	2005	14.27	14.33	1.04	0.526
140211	Formate dehydrogenase*	13.04	13.53	1.41	0.110	119730	None	85	1628	12.65	14.17	2.86	<0.001
6270	Oxidoreductase (GMC)*	9.80	10.16	1.29	0.184	None							

[a] To identify conserved sequences, the 12,438 *P. placenta* protein models represented on microarrays were aligned with all 10,048 v2 *P. chrysosporium* protein models using Timelogic harware (Active Motif, Carlsbad, CA) with accelerated double affine Smith-Waterman alignments. Scores, percent identities, and related alignment parameters for all genes are listed in Table S1 of the supplemental material. Normalized microarray data are presented as the average log_2 signal strength of three fully replicated experiments. Array-wide averaged signals (± standard deviations) for *P. chrysosporium* and *P. placenta* were 11.6 (1.6) and 10.9 (1.7), respectively. Significant accumulation (ratio) of transcripts in BMA relative to glucose (Glu) cultures was determined using the moderated *t* test (48) and associated false detection rates (4). Data are ranked according to the ratio, from highest to lowest. Underlined *P. chrysosporium* models correspond to genes with >50 cDNA tags in medium containing powdered oak (43). *, gene model whose proteins were identified in BMA filtrates by MS/MS. Table S1 in the supplemental material provides a summary of these data, and the complete MS/MS results are provided in Table S2.

chrysosporium and *P. placenta*, and these sequences are >87% identical to a methanol oxidase from the brown rot fungus *Gloeophyllum trabeum* (12).

Regulated and highly expressed *P. placenta* genes. The *P. placenta* genes whose transcripts accumulated >4-fold in glucose medium or in BMA medium (Fig. 2) differed markedly from the regulated *P. chrysosporium* genes (Fig. 1). Only five glycoside hydrolase-encoding genes were substantially upregulated in BMA medium (Fig. 2), but others were expressed at high levels in both glucose and BMA media, and still others encoded detectable extracellular protein irrespective of relatively low transcript levels. A total of 36 *P. placenta* GH proteins were flagged on the basis of high transcript levels and/or MS/MS identification (Table 3). Of the eight GH-encoding genes exceeding the genome-wide signal average (log_2, 10.9) by 2 standard deviations, none was upregulated >4-fold, and three were upregulated <2-fold in BMA medium (Table 3). In addition to high transcript levels, the likely importance of these genes was supported by LC-MS/MS identification of peptides in four cases (Table 3). Genes whose transcripts accumulated at significantly ($P < 0.01$) higher levels in glucose medium than in BMA medium included a GH47 mannosyl-oligosaccharide α-1,2-mannosidase (Ppl115593) and a GH20 chitooligosaccharidolytic β-*N*-acetylglucosaminidase (Ppl130398), which are possibly involved in protein modification and cell wall morphogenesis, respectively (Table 3).

The overall pattern of *P. placenta* GH regulation (Fig. 1 and 2), transcript levels (Table 3; see also Table S1 in the supplemental material), and mass spectrometry-based protein identification (see Tables S1 and S2) highlight the importance of hemicellulose hydrolysis with relatively few potential cellulases. Broadly defined, these putative hemicellulases include endo-β-1,4-mannosidases, endo-1,3(4)-β-glucanase, glucan 1,3-β-glucosidase, α-galactosidases, β-galactosidase, glucan 1,3-β-glucosidase, α-arabinofuranosidases, endoxylanases, β-mannosidase, α-1,2-mannosidases, galactan 1,3-β-galactosidase, and β-xylosidase. As mentioned above, the *P. placenta* genome lacks genes encoding exocellobiohydrolases or genes containing the cellulose binding module CBM1. Protein models assigned to the GH5 family and predicted to contain endoglucanase catalytic domains include Ppl103677, Ppl117690, and Ppl115648, which gave microarray signals of 11.7, 13.7, and 15.0, respectively (see Table S1). All showed >60% sequence identity to the *P. chrysosporium* endoglucanase designated EG38/36 (Pchr6458) (19, 51). The high transcript levels and protein scores observed for Ppl115648 support an important function, but in the absence of binding modules and exocellobiohydrolases, it is unclear how efficient cellulose hydrolysis proceeds. Apparent *P. placenta* orthologs of the *P. chrysosporium* GH12 endoglucanase EG28 (19) are transcribed in BMA (Ppl52805, log_2 of 9.23; Ppl121191, log_2 of 13.74), but the corresponding proteins were not detected by MS/MS.

Expression of *P. placenta* oxidoreductase genes differed sharply from *P. chrysosporium* genes. Transcripts of 23 genes accumulated >2-fold ($P < 0.001$) in BMA relative to glucose cultures, and peptides corresponding to four genes were detected in BMA filtrates (Table 4). With the exception of a polyphenol oxidase, Ppl114245, homologs were identified in all cases. However, only Ppl49605, a galacturonic acid reductase, and Ppl128830, a glucose-methanol-choline oxidoreductase (GMC oxidoreductase) distantly similar to glucose oxidase, were similarly regulated in the two fungi. Certain *P. chrysosporium* homologs were not regulated but

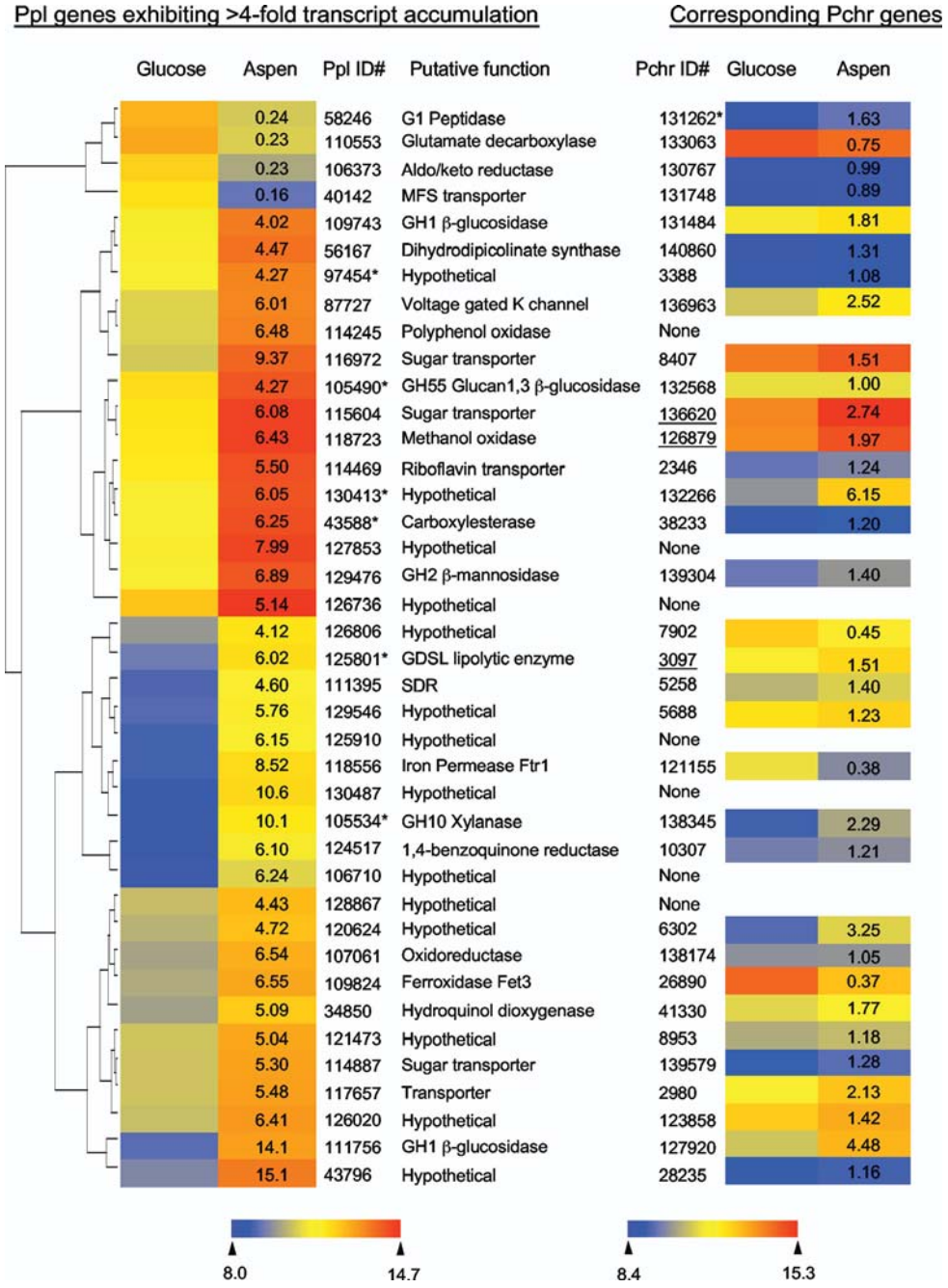

FIG. 2. Heat map showing hierarchical clustering of *P. placenta* genes exhibiting highly significant ($P < 0.001$) accumulation of transcripts in aspen-grown versus glucose-grown cultures. Numbers within boxes indicate the fold difference in transcripts in aspen versus glucose cultures. Only those *P. placenta* genes exceeding a 4-fold difference are shown. On right is a heat map showing transcript levels of the most closely related *P. chrysosporium* sequences or, in the absence of a clear homolog, labeled as "None." Protein IDs followed by asterisks correspond to peptides unambiguously identified by MS in filtrates from aspen-grown cultures. Scales below maps show $\log_2$-based signals. Underlined *P. chrysosporium* models correspond to genes with >50 cDNA tags in medium containing powdered oak (43).

still produced relatively high transcript levels in BMA medium. These included genes encoding a putative ferroxidase (Ppl109824), methanol oxidase (Ppl118723), and formate dehydrogenases (Ppl98518 and Ppl119730). Proteins corresponding to a copper radical oxidase (Ppl56703), an FAD-linked oxidoreductase (Ppl122772), and the above-mentioned GMC oxidoreductase (Ppl128830) were accompanied by relatively high transcript levels, but regulated expression levels that increased >2-fold were not observed. The *Postia* CRO protein is similar to three *P. chrysosporium* copper radical oxidases (CRO3, CRO4, and CRO5), with N-terminal repeats of a highly conserved WSC domain (55). None of the seven *P. chrysosporium* CRO proteins was detected by MS/MS in BMA cultures. Transcripts of the *P. placenta cro* genes, together with other putative oxidoreductases, were also detected by quantitative RT-PCR (Fig. 3).

TABLE 3. *P. placenta* genes encoding putative GHs with the highest transcript levels and/or positive MS/MS identification in BMA medium[a]

Postia placenta							*Phanerochaete chrysosporium*				
Model	Putative function	Allele	Signal (log_2) in:		Ratio	*P* value	Model	Signal (log_2) in:		Ratio	*P* value
			Glu	BMA				Glu	BMA		
115648	GH5 endo-1,4-β-glucanase*	108962	14.62	15.04	1.33	0.0012	6458	12.14	14.83	6.46	<0.001
119525	GH18 glycosidase	120960	14.81	14.83	1.02	0.7560	137237	9.00	9.71	1.64	0.0060
121831	GH5 endo-β-1,4-mannosidase*	134772	13.46	14.65	2.28	<0.001	140501	9.04	12.89	14.44	<0.001
112941	GH16 endo-1,3(4)-β-glucanase*	61809	12.66	14.58	3.79	<0.001	10833	11.77	13.65	3.68	0.0019
121713	GH5 glucan 1,3-β-glucosidase	46077	12.73	14.53	3.48	<0.001	121774	10.14	11.63	2.80	0.0092
117860	GH72 1,3-β-glucanosyltransferase*	118950	14.29	14.51	1.16	0.0206	6433	13.83	13.33	0.71	0.0232
134790	GH27 α-galactosidase*	98662	12.73	14.35	3.08	<0.001	134001	11.68	13.89	4.64	<0.001
94557	GH51 α-*N*-arabinofuranosidase*	None	13.06	14.31	2.38	<0.001	3651	12.20	12.96	1.70	0.0017
127993	GH35 β-galactosidase*	128101	13.65	14.17	1.43	0.0033	9466	11.26	11.69	1.34	0.0709
116267	GH55 glucan 1,3-β-glucosidase*	108648	13.35	14.16	1.75	<0.001	8072	12.03	13.98	3.88	0.0832
100251	GH51 α-*N*-arabinofuranosidase*	127046	12.31	14.05	3.34	<0.001	3651	12.20	12.96	1.70	0.00169
134924	GH31 α-glucosidase*	93878	13.33	13.51	1.13	0.0316	125462	12.38	12.62	1.18	0.373
113670	GH10 endo-1,4-β-xylanase*	134787	12.62	13.36	1.67	<0.001	138715	11.16	13.54	5.20	<0.001
57564	GH2 β-mannosidase*	56576	12.32	13.35	2.05	<0.001	135385	13.37	13.57	1.15	0.118
126692	GH79 glycosidase*	111332	11.71	13.34	3.10	<0.001	1999	10.55	11.88	2.52	0.0269
97540	GH37 trehalase*	115929	13.11	13.14	1.02	0.6770	140627	13.96	12.80	0.45	0.0254
112047	GH92 α-1,2-mannosidase*	116992	13.19	12.98	0.86	0.0134	3431	12.77	13.25	1.39	0.0109
126595	GH18 chitinase*	134923	12.59	12.86	1.21	0.1630	39872	14.02	13.71	0.81	0.172
112369	GH20 β-hexosaminidase*	61331	12.92	12.79	0.91	0.1450	37522	9.05	9.08	1.02	0.781
117345	GH15 glucoamylase*	113112	12.34	12.66	1.25	0.0420	138813	12.43	13.02	1.51	0.0771
120395	GH27 α-galactosidase*	None	11.50	12.54	2.06	<0.001	125033	12.22	12.91	1.61	0.0193
115593	GH47 Man(9)-α-mannosidase*	134925	13.48	12.51	0.51	<0.001	4550	11.62	13.44	3.52	<0.001
110809	GH43 galactan 1,3-β-galactosidase*	None	10.75	12.50	3.38	<0.001	297	10.64	11.10	1.38	0.0625
116199	GH5 glucan 1,3- β-glucosidase*	128425	12.15	12.47	1.24	0.0066	2220	12.43	13.66	2.35	0.00274
111730	GH28 polygalacturonase*	43189	10.53	12.40	3.66	<0.001	3805	10.90	14.57	12.70	<0.001
54405	GH16 endo-1,3(4)-β-glucanase*	135020	11.30	12.19	1.86	<0.001	123909	12.33	13.27	1.93	0.0283
127469	GH3 possible β-xylosidase*	51213	11.58	12.08	1.42	0.0047	9257	9.24	12.67	10.79	<0.001
107557	GH3 β-glucosidase*	None	11.95	12.02	1.06	0.5000	139063	14.70	14.55	0.90	0.599
46915	GH3 β-glucosidase*	95677	11.08	11.93	1.81	<0.001	129849	11.26	12.91	3.13	<0.001
105534	GH10 endo-1,4-β-xylanase*	None	8.38	11.71	10.06	<0.001	138345	9.23	10.43	2.29	0.014
55086	GH31 α-glucosidase*	19564	10.96	11.63	1.59	0.0014	968	11.64	12.73	2.12	0.0374
52194	GH13 α-amylase*	92881	11.45	11.62	1.13	0.1360	38357	13.86	13.60	0.83	0.141
62385	GH92 α-1,2-mannosidase*	48716	11.30	10.90	0.76	0.0278	133585	12.04	13.75	3.28	<0.001
130398	GH20 β-hexosaminidase*	134907	10.15	9.88	0.83	0.0052	140587	13.29	13.49	1.15	0.233
127046	GH51 α-*N*-arabinofuranosidase*	100251	9.50	9.81	1.24	0.0053	3651	12.20	12.96	1.70	0.00169
95568	GH5 endo-1,4-β-mannosidase*	None	8.91	9.52	1.52	<0.001	6579	12.43	13.67	2.36	0.00279

[a] Calculations are essentially the same as described for Table 2. The genes or alleles are listed in order of decreasing transcript levels. Detailed scores, e-values, and alignment parameters for the best *P. chrysosporium* hits are listed in Table S1 of the supplemental material. *, detection of peptides by LC-MS/MS in BMA medium filtrate (see Tables S1 and S2). Underlined *P. chrysosporium* models correspond to genes with >50 cDNA tags in medium containing powdered oak (43). Data are ranked according to *P. placenta* log_2 signals in BMA. The first eight genes exceeded the genome-wide average signal by 2 standard deviations (>14.24). Questionable GH51 models Ppl9457 and Ppl127046 lie within a 10-kb region of scaffold 110, and alignments suggest possible duplication or assembly error. The 3′ termini of *P. placenta* models GH20 Ppl130398 and GH10 Ppl113670 are problematic and require additional data and manual annotation. However, MS/MS protein assignments are based on reliable (5′) regions of these models.

DISCUSSION

Prior to genome sequencing, morphological and molecular evidence suggested a close relationship between *P. chrysosporium* and *P. placenta*, irrespective of their distinctly different decay patterns (21, 57). The availability of the genomes (36, 37) and the broad proteome comparisons reported here largely underscore this close relationship. However, closer comparative transcriptome and secretome analyses illuminate complex and divergent physiological mechanisms employed in lignocellulose degradation by these model wood decay fungi.

BlastP comparisons of *P. chrysosporium* proteins showed significant alignments for 71% of the 12,438 unique *P. placenta* models. These findings are sensitive to changes in the threshold e-value. For example, at an e-value of 10^{-10}, 66% of the 12,438 *P. placenta* models were matched to at least one *P. chrysosporium* model. Our analysis involved identification of the best possible alignments using *P. placenta* protein sequences as a query to all *P. chrysosporium* targets, and this approach provides an overall measure of relatedness. The vast majority of best hit pairs are also the best reciprocal hits (6) as determined by additional BlastP analysis and manual inspections of all regulated genes, but the complete *P. chrysosporium* protein database was not queried against all *P. placenta* protein models. Draft genomes and automated annotations always contain assembly, model, and sequence errors. In addition, *P. placenta* allelism and the prevalence of *P. chrysosporium* extended gene families advise cautious assignment of orthologous pairs. For example, the most highly expressed and upregulated member of the GH5 family in *P. placenta*, Ppl115648, is most closely related to Pchr6458 (Table 3; see also Table S1 in the supplemental material), but it also shares sequence similarity (27% identity, 70% coverage, score of 202; e-value, 2.2

TABLE 4. *P. placenta* genes encoding putative oxidoreductases upregulated >2-fold in BMA medium relative to glucose medium or matched to MS/MS-derived peptide sequences[a]

Postia placenta							*Phanerochete chrysosporium*						
Model	Putative function	Allele	Signal (log_2) in:		Ratio	*P* value	Model	Pairwise alignment		Signal (log_2) in:		Ratio	*P* value
			Glu	BMA				% ID	Score	Glu	BMA		
109824	Ferroxidase Fet3	134624	10.01	12.72	6.55	<0.001	26890	68	2275	14.40	12.95	0.37	0.0124
107061	Oxidoreductase	51016	9.90	12.61	6.54	<0.001	138174	61	1126	10.07	10.14	1.05	0.698
114245	Polyphenol oxidase	109291	10.62	13.32	6.48	<0.001	None						
118723	Alcohol oxidase	129841	11.76	14.44	6.43	<0.001	126879	88	3090	13.77	14.74	1.97	0.0199
124517	1,4-Benzoquinone reductase	64069	8.41	11.02	6.10	<0.001	10307	74	821	9.77	10.05	1.21	0.11
34850	Hydroquinol 1,2-dioxygenase	87645	9.86	12.21	5.09	<0.001	41330	71	943	11.20	12.02	1.77	0.0252
111395	Short chain dehydrogenase	64558	8.95	11.15	4.60	<0.001	5258	78	404	10.63	11.12	1.40	0.0162
98518	Formate dehydrogenase	89897	10.12	12.03	3.76	<0.001	140211	82	1578	13.04	13.53	1.41	0.106
61437	Aldehyde dehydrogenase	89252	8.75	10.57	3.51	<0.001	133924	33	483	12.25	11.03	0.43	0.0143
46931	Laccase (fragment)	111314	10.0	11.65	3.15	0.007	10581	40	206	8.6	8.67	1.05	0.45
108989	2-Nitropropane dioxygenase	None	11.60	13.20	3.04	<0.001	218	75	1412	11.98	12.12	1.10	0.258
113908	Acireductone dioxygenase	63611	10.51	12.11	3.03	<0.001	123880	53	508	12.90	12.82	0.94	0.491
24981	Hydroquinol 1,2-dioxygenase	107881	11.60	13.13	2.88	<0.001	136660	79	984	11.34	11.89	1.46	0.0769
119730	Formate dehydrogenase	None	12.65	14.17	2.86	<0.001	140211	85	1628	13.04	13.53	1.41	0.106
51235	P450*	20385	11.73	13.22	2.81	<0.001	1200	55	1355	11.40	11.51	1.08	0.38
43234	α-Aminoadipate reductase	None	10.83	12.29	2.75	<0.001	6025	29	851	9.48	9.52	1.03	0.605
61079	Chloroperoxidase	25391	8.97	10.42	2.72	<0.001	3274	63	922	11.07	11.37	1.23	0.0271
116179	Short chain dehydrogenase	None	11.22	12.57	2.55	<0.001	132770	69	956	9.71	10.05	1.27	0.0673
49605	Galacturonic acid reductase	61601	10.07	11.41	2.53	<0.001	6771	76	1544	10.09	11.71	3.09	0.0016
115028	Aryl alcohol dehydrogenase	89343	11.56	12.69	2.18	<0.001	128103	71	1459	10.45	10.91	1.38	0.00751
108358	2-Nitropropane dioxygenase	56793	10.01	11.08	2.11	<0.001	4432	87	1486	10.89	11.16	1.21	0.0874
126817	Flavin monooxygenase	104883	10.54	11.62	2.11	0.008	6291	57	1825	11.87	12.06	1.14	0.47
111823	Oxidoreductase	120225	12.67	13.71	2.05	<0.001	2284	68	1305	8.49	8.83	1.26	0.036
56703	CRO5*	99632	12.73	13.60	1.82	0.0022	8882	66	3651	12.72	12.55	0.89	0.277
122772	OR FAD linked*	114192	13.22	14.07	1.80	<0.001	138076	53	1151	8.93	8.85	0.95	0.527
128830	Glucose oxidase-like*	None	13.25	13.11	0.91	0.3910	131961	31	734	12.32	12.20	0.93	0.349

[a] Calculations are essentially the same as described for Table 2. The *P. chrysosporium* homolog with the highest alignment score was reported for each *P. placenta* gene. Scores, percent identity, and related alignment parameters for all genes are listed in Table S1 of the supplemental material. With one exception (galacturonic acid reductase), transcripts of the corresponding *P. chrysosporium* gene exhibited relatively lower accumulation ratios and a concomitantly higher false discovery rate (4) probability (far right column). Underlined *P. chrysosporium* models correspond to genes with >50 cDNA tags in medium containing powdered oak (43). Data are ranked according to the *P. placenta* ratio, from highest to lowest. *, detection of corresponding peptides by MS/MS in BMA medium filtrate.

e^{-20}) with Pchr4361. These *P. chrysosporium* genes encode well-characterized β-1,4-endoglucanase isozymes EG38/36 (Pchr6458) and EG44 (Pchr4361), both of which contain a cellulose binding domain (CBM1). In contrast, Ppl115648 does not possess a binding module, and its catalytic function has yet to be determined. Of course, proteins with similar sequences may have divergent functions, as is the case for Ppl46931 and its closest homolog, Pchr10581. Careful examination of these sequences revealed that Ppl46931 likely encodes a phenol oxidase (laccase), whereas laccases are absent from the *P. chrysosporium* genome, and Pchr10581 corresponds to MCO4 (34), a multicopper oxidase predicted to have ferroxidase-like activity (24, 34).

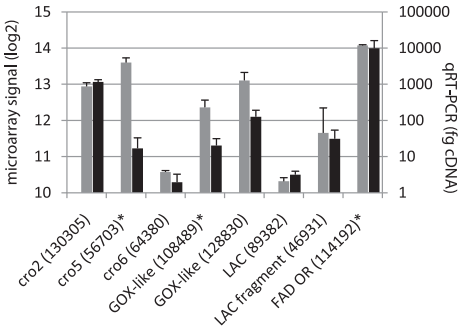

FIG. 3. Transcript levels of *P. placenta* genes encoding copper radical oxidases (Ppl130305, Ppl56703, and Ppl64380), GMC oxidoreductases with distant similarity to glucose oxidase (GOX; Ppl108489 and Ppl128830), an intact laccase (Ppl89382), a truncated laccase model (Ppl46931), and the highly expressed FAD-dependent oxidoreductase Ppl114192 (Table 4). Gray bars and the left axis represent log_2 microarray signals. Blackened bars and the right axis represent cDNA as determined by competitive RT-PCR. Asterisks indicate protein models whose peptides were identified in concentrated filtrates of aspen-grown cultures.

After 5 days of growth in medium containing ball-milled aspen as the sole carbon source, the overall pattern of gene expression in *P. chrysosporium* and *P. placenta* cultures revealed an impressive array of extracellular glycoside hydrolases. MS/MS-identified proteins and corresponding transcript patterns clearly demonstrated expression of multiple extracellular endoglucanases and exocellobiohydrolases by *P. chrysosporium*. These observations strongly support a conventional system of synergistically acting enzymes. In contrast, hemicellulases dominated as the more highly expressed *P. placenta* genes under these same culture conditions. As degradation advances beyond 5 days, these expression patterns would likely shift. Systematic time course analyses by microarray and mass spectrometry, while costly, would illuminate such patterns.

Our microarray-based transcript profiles for *P. chrysosporium* differ substantially from those of Sato et al. (43), who

used deep RNA sequencing (cDNA pyrosequencing). Comparing their 293 genes, which gave rise to >15 RNA tags, to our microarray signals results in a low correlation coefficient, 0.13. Very different culture conditions were employed, e.g., water-extracted oak powder versus ball-milled aspen and 6-day stationary cultures versus 5-day shake flasks. Still, although the data of Sato et al. were not intended to identify and measure regulated expression, we note that of the 32 most highly upregulated genes in BMA (Fig. 1), 14 were also judged as highly expressed in oak culture, with each having >50 tags.

To highlight comparisons of the cellulolytic systems, experiments were focused on short-term growth with ball-milled aspen as sole carbon source. This complex lignocellulose perhaps more closely mimics natural substrates relative to defined media containing glucose or pure microcrystalline cellulose (36, 45, 52, 53). However, submerging finely ground wood in basal salts hardly replicates the decay typically occurring in nature. Defined culture conditions allow straightforward harvesting of mycelia and extracellular enzymes, whereas in the present case the developing hyphae become intractably bound to the substrate. Simple measurements of biomass accumulation are difficult, and proteins may remain bound. In this connection, we observed modest upregulation of two lignin peroxidase genes (Table 2), but no enzyme activity or peptide sequences were detected for lignin peroxidases, manganese peroxidases, or glyoxal oxidase in *P. chrysosporium* cultures. The absence of these activities and of MS-detectable peptides persists for at least 14 days (data not shown).

Although these well-known components of the *P. chrysosporium* ligninolytic system were not detected in BMA cultures, high expression levels of methanol oxidase genes were observed in *P. chrysosporium* and *P. placenta* cultures (Table 4). In the brown rot fungus *G. trabeum*, this GMC oxidase is cell wall associated and thought to play an important role in peroxide generation (12). Although lignin metabolism differs substantially between white rot and brown rot fungi, lignin demethoxylation occurs in both types of decay. Methanol oxidation may be an important reaction generating peroxide and formaldehyde, and the observed high expression of formate dehydrogenases in both fungi may reflect the complete metabolism of methanol.

Demethoxylation substrates may not be limited to lignin moieties, and some evidence suggests that substituted hydroquinones, known to be synthesized by several brown rot fungi, play a role in driving Fenton chemistry (11, 46). The biosynthesis of hydroquinones, such a 2,5-dimethoxy-1,4-benzoquinone (2,5-DMHQ), has not been experimentally established but likely involves conversions of aromatic amino acids. In this connection, we observed significant upregulation ($P < 0.001$, >2-fold) of *P. placenta* genes encoding phenylalanine ammonium lyase (Ppl112824), 4-coumarate coenzyme A (CoA) ligase (Ppl43879), and an *O*-methyl transferase (Ppl47451) in BMA cultures, while the *P. chrysosporium* orthologs were downregulated or unchanged (4-coumarate-CoA ligase) under the same conditions (see Table S1 in the supplemental material). Beyond biosynthesis of hydroquinones, we also observed upregulation of a potential quinate transporter, Ppl44553, although transcripts of the putative *P. chrysosporium* ortholog, Pchr138158, also accumulated in BMA medium.

The mechanisms controlling extracellular Fenton reactions have been the subject of considerable debate (reviewed in references 2 and 17). Our *P. placenta* results support a hydroquinone-driven system and address the central question of quinone reduction. Specifically, we observed significant upregulation of 1,4-benzoquinone reductase (Ppl124517) in *P. placenta* BMA cultures, but not in *P. chrysosporium* cultures. Not only are benzoquinone reductase (Ppl124517) transcript levels significantly upregulated in *Postia* BMA cultures, but so too are those of a hydroquinol dioxygenase (Ppl 34850). Studies with *Phanerochaete* suggest roles for both a quinone reductase (8) and a hydroquinol dioxygenase (42) in aromatic metabolism of lignin fragments. Benzoquinone reductase in *Postia* may have dual roles, one in generating reactive oxygen species and a second role in aromatic metabolism in conjunction with hydroquinol dioxygenase. In addition, a tyrosinase-encoding gene (polyphenol oxidase, Ppl114245) and a laccase (Ppl46931), neither having a *P. chrysosporium* ortholog, were also significantly upregulated in BMA medium. The latter enzyme has been suggested to support a redox system via oxidation of hydroquinones (16, 18).

Other *P. placenta* enzymes potentially involved in extracellular peroxide generation include a copper radical oxidase (Ppl56703), an FAD-linked oxidoreductase (Ppl122772), and a glucose oxidase-like protein (Ppl128830) (Table 4). Based on transcripts and mass spectrometry, secretion of these proteins is firmly established, but their precise activities, especially substrate preferences, remain to be determined.

Further highlighting the physiological distinctions between *P. chrysosporium* and *P. placenta* are gene expression patterns related to iron homeostasis, crucial to a Fenton system. The importance of hydroquinone-driven Fenton chemistry in *P. placenta* remains unclear because, under certain culture conditions, this fungus secretes high levels of oxalate (29), and Fe^{3+}-oxalate chelates are poorly reducible by hydroquinones (27). In our BMA medium, relatively low oxalate concentrations were detected (<50 μM) for both *P. chrysosporium* and *P. placenta*. Under these conditions, iron acquisition systems of the two species exhibited distinctly different expression patterns, with genes encoding ferroxidase and iron permease substantially upregulated in *P. placenta* and downregulated in *P. chrysosporium* (Fig. 2). Conversely, a membrane-anchored ferric reductase-like gene (Pchr1139) was highly expressed in *P. chrysosporium*, while the putative *P. placenta* ortholog (Ppl130043) was expressed at low levels (Table 2). Extracellular iron reductase activity in *P. chrysosporium* has been ascribed to low-molecular-weight glycopeptides GLP1 and GLP2 (49), but their $\log_2$ microarray signals are relatively low in BMA medium at 10.4 and 11.38, respectively. Four putative orthologs are present in the *P. placenta* genome, two of which gave high signals (Ppl128371, 12.57; Ppl128976, 14.72). Accordingly, a role for these glycoproteins in a *P. placenta* Fenton system is possible.

Assessing the role(s) of hypothetical proteins remains problematic and especially challenging for *P. placenta*, which has a significantly higher number of "hypotheticals" expressed in BMA medium relative to *P. chrysosporium*. Several *Postia* hypotheticals (Ppl127853, Ppl126736, Ppl125910, Ppl130487, Ppl106710, and Ppl128867) have no apparent homologs in *P. chrysosporium* and, significantly, are highly upregulated in BMA medium (Fig. 2). In other cases (Ppl97454, Ppl12680,

Ppl12147, and Ppl4379), putative orthologs were identified but the *P. placenta* gene was more highly expressed and/or upregulated relative to the *P. chrysosporium* gene. Peptides matching Ppl97454, but not its *P. chrysosporium* ortholog Pchr3388, were detected in culture filtrates. In contrast, both Ppl130413 and Pchr132266 had relatively high transcript levels in BMA medium, and the presence of the corresponding extracellular proteins was confirmed by mass spectrometry (Fig. 2). The *P. placenta* and *P. chrysosporium* genomes feature thousands of hypothetical proteins. Structural features of these protein models are occasionally informative, e.g., secretion signals, but often unreliable and unfulfilling. Transcript and secretome profiles as described here will help to focus future research attention on more manageable subsets of functional genes.

ACKNOWLEDGMENTS

This work was supported by the National Research Initiative of the USDA Cooperative State Research, Education and Extension Service, grant number 2007-35504-18257 to the Forest Products Laboratory, by Office of Science U.S. Department of Energy contract DE-AC02-05CH11231 to the Joint Genome Institute, and by the DOE Great Lakes Bioenergy Research Center (DOE Office of Science BER DE-FC02-07ER64494).

REFERENCES

1. **Abbas, A., H. Koc, F. Liu, and M. Tien.** 2004. Fungal degradation of wood: initial proteomic analysis of extracellular proteins of *Phanerochaete chrysosporium* grown on oak substrate. Curr. Genet. **47:**49–56.
2. **Baldrian, P., and V. Valaskova.** 2008. Degradation of cellulose by basidiomycetous fungi. FEMS Microbiol. Rev. **32:**501–521.
3. **Bao, W., E. Lymar, and V. Renganathan.** 1994. Optimization of cellobiose dehydrogenase and β-glucosidase production by cellulose-degrading cultures of *Phanerochaete chrysosporium*. Appl. Biochem. Biotechnol. **42:**642–646.
4. **Benjamini, Y., and Y. Hochberg.** 1995. Controlling the false discovery rate: a practical and powerful approach to multiple testing. J. R. Stat. Soc. B **57:**289–300.
5. **Binder, M., D. Hibbett, K. H. Larsson, E. Larsson, and E. Langer.** 2005. The phylogenetic distribution of resupinate forms in the homobasidiomycetes. Syst. Biodivers. **3:**113–157.
6. **Bork, P., T. Dandekar, Y. Diaz-Lazcoz, F. Eisenhaber, M. Huynen, and Y. Yuan.** 1998. Predicting function: from genes to genomes and back. J. Mol. Biol. **283:**707–725.
7. **Brazma, A., P. Hingamp, J. Quackenbush, G. Sherlock, P. Spellman, C. Stoeckert, J. Aach, W. Ansorge, C. A. Ball, H. C. Causton, T. Gaasterland, P. Glenisson, F. C. Holstege, I. F. Kim, V. Markowitz, J. C. Matese, H. Parkinson, A. Robinson, U. Sarkans, S. Schulze-Kremer, J. Stewart, R. Taylor, J. Vilo, and M. Vingron.** 2001. Minimum information about a microarray experiment (MIAME)-toward standards for microarray data. Nat. Genet. **29:**365–371.
8. **Buswell, J. A., S. Hamp, and K. E. Eriksson.** 1979. Intracellular quinone reduction in *Sporotrichum pulverulentum* by NAD(P)H:quinone oxidoreductase: possible role in vanillic acid catabolism. FEBS Lett. **108:**229–232.
9. **Cantarel, B. L., P. M. Coutinho, C. Rancurel, T. Bernard, V. Lombard, and B. Henrissat.** 2009. The Carbohydrate-Active enZymes database (CAZy): an expert resource for glycogenomics. Nucleic Acids Res. **37:**D233–D238.
10. **Cohen, R., K. A. Jensen, C. J. Houtman, and K. E. Hammel.** 2002. Significant levels of extracellular reactive oxygen species produced by brown rot basidiomycetes on cellulose. FEBS Lett. **531:**483–488.
11. **Cohen, R., M. R. Suzuki, and K. E. Hammel.** 2004. Differential stress-induced regulation of two quinone reductases in the brown rot basidiomycete *Gloeophyllum trabeum*. Appl. Environ. Microbiol. **70:**324–331.
12. **Daniel, G., J. Volc, L. Filonova, O. Plihal, E. Kubatova, and P. Halada.** 2007. Characteristics of *Gloeophyllum trabeum* alcohol oxidase, an extracellular source of H_2O_2 in brown rot decay of wood. Appl. Environ. Microbiol. **73:**6241–6253.
13. **Duranova, M., J. Hirsch, K. Kolenova, and P. Biely.** 2009. Fungal glucuronoyl esterases and substrate uronic acid recognition. Biosci. Biotechnol. Biochem. **73:**2483–2487.
14. **Duranova, M., S. Spanikova, H. A. Wosten, P. Biely, and R. P. de Vries.** 2009. Two glucuronoyl esterases of *Phanerochaete chrysosporium*. Arch. Microbiol. **191:**133–140.
15. **Eriksson, K.-E. L., R. A. Blanchette, and P. Ander.** 1990. Microbial and enzymatic degradation of wood and wood components. Springer-Verlag, Berlin, Germany.
16. **Gomez-Toribio, V., A. B. Garcia-Martin, M. J. Martinez, A. T. Martinez, and F. Guillen.** 2009. Induction of extracellular hydroxyl radical production by white rot fungi through quinone redox cycling. Appl. Environ. Microbiol. **75:**3944–3953.
17. **Goodell, B.** 2003. Brown rot fungal degradation of wood: our evolving view, p. 97–118. *In* B. Goodell, D. Nicholas, and T. Schultz (ed.), Wood deterioration and preservation. American Chemical Society, Washington, DC.
18. **Guillen, F., M. J. Martinez, C. Munoz, and A. T. Martinez.** 1997. Quinone redox cycling in the ligninolytic fungus *Pleurotus eryngii* leading to extracellular production of superoxide anion radical. Arch. Biochem. Biophys. **339:**190–199.
19. **Henriksson, G., A. Nutt, H. Henriksson, B. Pettersson, J. Stahlberg, G. Johansson, and G. Pettersson.** 1999. Endoglucanase 28 (Cel12A), a new *Phanerochaete chrysosporium* cellulase. Eur. J. Biochem. **259:**88–95.
20. **Hibbett, D. S., M. Binder, J. F. Bischoff, M. Blackwell, P. F. Cannon, O. E. Eriksson, S. Huhndorf, T. James, P. M. Kirk, R. Lucking, H. Thorsten Lumbsch, F. Lutzoni, P. B. Matheny, D. J. McLaughlin, M. J. Powell, S. Redhead, C. L. Schoch, J. W. Spatafora, J. A. Stalpers, R. Vilgalys, M. C. Aime, A. Aptroot, R. Bauer, D. Begerow, G. L. Benny, L. A. Castlebury, P. W. Crous, Y. C. Dai, W. Gams, D. M. Geiser, G. W. Griffith, C. Gueidan, D. L. Hawksworth, G. Hestmark, K. Hosaka, R. A. Humber, K. D. Hyde, J. E. Ironside, U. Koljalg, C. P. Kurtzman, K. H. Larsson, R. Lichtwardt, J. Longcore, J. Miadlikowska, A. Miller, J. M. Moncalvo, S. Mozley-Standridge, F. Oberwinkler, E. Parmasto, V. Reeb, J. D. Rogers, C. Roux, L. Ryvarden, J. P. Sampaio, A. Schussler, J. Sugiyama, R. G. Thorn, L. Tibell, W. A. Untereiner, C. Walker, Z. Wang, A. Weir, M. Weiss, M. M. White, K. Winka, Y. J. Yao, and N. Zhang.** 2007. A higher-level phylogenetic classification of the fungi. Mycol. Res. **111:**509–547.
21. **Hibbett, D. S., and M. J. Donoghue.** 2001. Analysis of character correlations among wood decay mechanisms, mating systems, and substrate ranges in homobasidiomycetes. Syst. Biol. **50:**215–242.
22. **Higham, C. W., D. Gordon-Smith, C. E. Dempsey, and P. M. Wood.** 1994. Direct 1H NMR evidence for conversion of beta-D-cellobiose to cellobionolactone by cellobiose dehydrogenase from *Phanerochaete chrysosporium*. FEBS Lett. **351:**128–132.
23. **Highley, T. L.** 1973. Influence of carbon source on cellulase activity of white rot and brown rot fungi. Wood Fiber **5:**50–58.
24. **Hoegger, P. J., S. Kilaru, T. Y. James, J. R. Thacker, and U. Kües.** 2006. Phylogenetic comparison and classification of laccase and related multicopper oxidase protein sequences. FEBS J. **273:**2308–2326.
25. **Hunt, C., W. Kenealy, E. Horn, and C. J. Houtman.** 2004. A biopulping mechanism: creation of acid groups on fiber. Holzforschung **58:**434–439.
26. **Irizarry, R. A., B. Hobbs, F. Collin, Y. D. Beazer-Barclay, K. J. Antonellis, U. Scherf, and T. P. Speed.** 2003. Exploration, normalization, and summaries of high density oligonucleotide array probe level data. Biostatistics **4:**249–264.
27. **Jensen, K. A., Jr., C. J. Houtman, Z. C. Ryan, and K. E. Hammel.** 2001. Pathways for extracellular Fenton chemistry in the brown rot basidiomycete *Gloeophyllum trabeum*. Appl. Environ. Microbiol. **67:**2705–2711.
28. **Jiang, M., X. Li, L. Zhang, H. Feng, and Y. Zhang.** 2009. Gene expression analysis of *Phanerochaete chrysosporium* during the transition time from primary growth to secondary metabolism. J. Microbiol. **47:**308–318.
29. **Kaneko, S., K. Yoshitake, S. Itakura, H. Tanaka, and A. Enoki.** 2005. Relationship between production of hydroxyl radicals and degradation of wood, crystalline cellulose, and lignin-related compound or accumulation of oxalic acid in cultures of brown rot fungi. J. Wood Sci. **51:**262–269.
30. **Karkehabadi, S., H. Hansson, S. Kim, K. Piens, C. Mitchinson, and M. Sandgren.** 2008. The first structure of a glycoside hydrolase family 61 member, Cel61B from *Hypocrea jecorina*, at 1.6 Å resolution. J. Mol. Biol. **383:**144–154.
31. **Kersten, P. J.** 1990. Glyoxal oxidase of *Phanerochaete chrysosporium*: its characterization and activation by lignin peroxidase. Proc. Natl. Acad. Sci. U. S. A. **87:**2936–2940.
32. **Kersten, P. J., and T. K. Kirk.** 1987. Involvement of a new enzyme, glyoxal oxidase, in extracellular H_2O_2 production by *Phanerochaete chrysosporium*. J. Bacteriol. **169:**2195–2201.
33. **Kirk, T. K., and R. L. Farrell.** 1987. Enzymatic "combustion": the microbial degradation of lignin. Annu. Rev. Microbiol. **41:**465–505.
34. **Larrondo, L., B. Gonzalez, D. Cullen, and R. Vicuna.** 2004. Characterization of a multicopper oxidase gene cluster in *Phanerochaete chrysosporium* and evidence for altered splicing of the *mco* transcript. Microbiology **150:**2775–2783.
35. **Martin, S. E., J. Shabanowitz, D. F. Hunt, and J. A. Marto.** 2000. Subfemtomole MS and MS/MS peptide sequence analysis using nano-HPLC-ESI Fourier transform ion cyclotron resonance mass spectrometry. Anal. Chem. **72:**4266–4274.
36. **Martinez, D., J. Challacombe, I. Morgenstern, D. Hibbett, M. Schmoll, C. P. Kubicek, P. Ferreira, F. J. Ruiz-Duenas, A. T. Martinez, P. Kersten, K. E. Hammel, A. Vanden Wymelenberg, J. Gaskell, E. Lindquist, G. Sabat, S. S. Bondurant, L. F. Larrondo, P. Canessa, R. Vicuna, J. Yadav, H. Doddapaneni, V. Subramanian, A. G. Pisabarro, J. L. Lavin, J. A. Oguiza, E. Master, B. Henrissat, P. M. Coutinho, P. Harris, J. K. Magnuson, S. E. Baker, K. Bruno, W. Kenealy, P. J. Hoegger, U. Kues, P. Ramaiya, S. Lucas, A.**

Salamov, H. Shapiro, H. Tu, C. L. Chee, M. Misra, G. Xie, S. Teter, D. Yaver, T. James, M. Mokrejs, M. Pospisek, I. V. Grigoriev, T. Brettin, D. Rokhsar, R. Berka, and D. Cullen. 2009. Genome, transcriptome, and secretome analysis of wood decay fungus *Postia placenta* supports unique mechanisms of lignocellulose conversion. Proc. Natl. Acad. Sci. U. S. A. **106:**1954–1959.

37. **Martinez, D., L. F. Larrondo, N. Putnam, M. D. Sollewijn Gelpke, K. Huang, J. Chapman, K. G. Helfenbein, P. Ramaiya, J. C. Detter, F. Larimer, P. M. Coutinho, B. Henrissat, R. Berka, D. Cullen, and D. Rokhsar.** 2004. Genome sequence of the lignocellulose degrading fungus *Phanerochaete chrysosporium* strain RP78. Nat. Biotechnol. **22:**695–700.
38. **Minami, M., O. Kureha, M. Mori, H. Kamitsuji, K. Suzuki, and T. Irie.** 2007. Long serial analysis of gene expression for transcriptome profiling during the initiation of ligninolytic enzymes production in *Phanerochaete chrysosporium*. Appl. Microbiol. Biotechnol. **75:**609–618.
39. **Nesvizhskii, A. I., A. Keller, E. Kolker, and R. Aebersold.** 2003. A statistical model for identifying proteins by tandem mass spectrometry. Anal. Chem. **75:**4646–4658.
40. **Niemenmaa, O., A. Uusi-Rauva, and A. Hatakka.** 2007. Demethoxylation of $O_{14}CH_3$-labelled lignin model compounds by the brown rot fungi *Gloeophyllum trabeum* and *Poria* (*Postia*) *placenta*. Biodegradation **19:**555–565.
41. **Ravalason, H., G. Jan, D. Molle, M. Pasco, P. M. Coutinho, C. Lapierre, B. Pollet, F. Bertaud, M. Petit-Conil, S. Grisel, J. C. Sigoillot, M. Asther, and I. Herpoel-Gimbert.** 2008. Secretome analysis of *Phanerochaete chrysosporium* strain CIRM-BRFM41 grown on softwood. Appl. Microbiol. Biotechnol. **80:**719–733.
42. **Rieble, S., D. Joshi, and M. H. Gold.** 1994. Purification and characterization of a 1,2,4-trihydroxybenzene 1,2-dioxygenase from the basidiomycete *Phanerohchaete chrysosporium*. J. Bacteriol. **176:**4838–4844.
43. **Sato, S., F. A. Feltus, P. Iyer, and M. Tien.** 2009. The first genome-level transcriptome of the wood-degrading fungus *Phanerochaete chrysosporium* grown on red oak. Curr. Genet. **55:**273–286.
44. **Sato, S., F. Liu, H. Koc, and M. Tien.** 2007. Expression analysis of extracellular proteins from *Phanerochaete chrysosporium* grown on different liquid and solid substrates. Microbiology **153:**3023–3033.
45. **Shimizu, M., N. Yuda, T. Nakamura, H. Tanaka, and H. Wariishi.** 2005. Metabolic regulation at the tricarboxylic acid and glyoxylate cycles of the lignin-degrading basidiomycete *Phanerochaete chrysosporium* against exogenous addition of vanillin. Proteomics **5:**3919–3931.
46. **Shimokawa, T., M. Nakamura, N. Hayashi, and M. Ishihara.** 2004. Production of 2,5-dimethoxyhydroquinone by the brown rot fungus *Serpuyla lacrymans* to drive extracellular Fenton reaction. Holzforschung **58:**305–310.
47. **Smith, T. F., and M. S. Waterman.** 1981. Identification of common molecular subsequences. J. Mol. Biol. **147:**195–197.
48. **Smyth, G. K.** 2004. Linear models and empirical bayes methods for assessing differential expression in microarray experiments. Stat. Appl. Genet. Mol. Biol. **3:**Article3.
49. **Tanaka, H., G. Yoshida, Y. Baba, K. Matsumura, H. Wasada, J. Murata, M. Agawa, S. Itakura, and A. Enoki.** 2007. Characterization of a hydroxyl-radical-producing glycoprotein and its presumptive genes from the white rot basidiomycete *Phanerochaete chrysosporium*. J. Biotechnol. **128:**500–511.
50. **Tien, M., and T. K. Kirk.** 1984. Lignin-degrading enzyme from *Phanerochaete chrysosporium*: purification, characterization, and catalytic properties of a unique H_2O_2-requiring oxygenase. Proc. Natl. Acad. Sci. U. S. A. **81:**2280–2284.
51. **Uzcategui, E., G. Johansson, B. Ek, and G. Pettersson.** 1991. The 1,4-D-glucan glucanohydrolases from *Phanerochaete chrysosporium*. Re-assessment of their significance in cellulose degradation mechanisms. J. Biotechnol. **21:**143–160.
52. **Vanden Wymelenberg, A., J. Gaskell, M. D. Mozuch, P. Kersten, G. Sabat, D. Martinez, and D. Cullen.** 2009. Transcriptome and secretome analysis of *Phanerochaete chrysosporium* reveal complex patterns of gene expression. Appl. Environ. Microbiol. **75:**4058–4068.
53. **Vanden Wymelenberg, A., P. Minges, G. Sabat, D. Martinez, A. Aerts, A. Salamov, I. Grigoriev, H. Shapiro, N. Putnam, P. Belinky, C. Dosoretz, J. Gaskell, P. Kersten, and D. Cullen.** 2006. Computational analysis of the *Phanerochaete chrysosporium* v2.0 genome database and mass spectrometry identification of peptides in ligninolytic cultures reveals complex mixtures of secreted proteins. Fungal Genet. Biol. **43:**343–356.
54. **Vanden Wymelenberg, A., G. Sabat, D. Martinez, A. S. Rajangam, T. T. Teeri, J. Gaskell, P. J. Kersten, and D. Cullen.** 2005. The *Phanerochaete chrysosporium* secretome: database predictions and initial mass spectrometry peptide identifications in cellulose-grown medium. J. Biotechnol. **118:**17–34.
55. **Vanden Wymelenberg, A., G. Sabat, M. D. Mozuch, P. Kersten, D. Cullen, and R. A. Blanchette.** 2006. Structure, organization, and transcriptional regulation of a family of copper radical oxidase genes in the lignin-degrading basidiomycete *Phanerochaete chrysosporium*. Appl. Environ. Microbiol. **72:**4871–4877.
56. **Wariishi, H., K. Valli, and M. H. Gold.** 1992. Mn oxidation by manganese peroxidase from *Phanerochaete chrysosporium*: kinetic mechanisms and role of chelators. J. Biol. Chem. **267:**23688–23695.
57. **Worrall, J. J., S. E. Anagnost, and R. A. Zabel.** 1997. Comparison of wood decay among diverse lignicolous fungi. Mycologia **89:**199–219.
58. **Xu, G., and B. Goodell.** 2001. Mechanisms of wood degradation by brown rot fungi: chelator-mediated cellulose degradation and binding of iron by cellulose. J. Biotechnol. **87:**43–57.
59. **Yelle, D. J., J. Ralph, F. Lu, and K. E. Hammel.** 2008. Evidence for cleavage of lignin by a brown rot basidiomycete. Environ. Microbiol. **10:**1844–1849.
60. **Yoshida, M., K. Igarashi, M. Wada, S. Kaneko, N. Suzuki, H. Matsumura, N. Nakamura, H. Ohno, and M. Samejima.** 2005. Characterization of carbohydrate-binding cytochrome b_{562} from the white rot fungus *Phanerochaete chrysosporium*. Appl. Environ. Microbiol. **71:**4548–4555.